

Astrophysical S -factor of the $d(p,\gamma)^3\text{He}$ process by effective field theory

H. Sadeghi¹⁾ H. Khalili M. Godarzi

Department of Physics, Faculty of Science, Arak University, Arak 8349-8-38156, Iran

Abstract: We summarize the recent effective field theory (EFT) studies of low-energy electroweak reactions of astrophysical interest, relevant to big-bang nucleosynthesis. The zero energy astrophysical $S(0)$ factor for the thermal proton radiative capture by deuteron is calculated with pionless EFT. The astrophysical $S(0)$ factor is accurately determined to be $S(0) = 0.243 \text{ eV}\cdot\text{b}$ up to the leading order (LO). At zero energies, magnetic transition M_1 gives the dominant contribution. The M_1 amplitude is calculated up to the LO. A good, quantitative agreement between theoretical and experimental results is found for all observables. The demonstrations of cutoff independent calculation have also been presented.

Key words: proton-deuteron radiative capture, effective field theory, cross section, astrophysical S -factor

PACS: 21.45.lv, 24.70.ls, 25.40.Lw **DOI:** 10.1088/1674-1137/37/4/044102

1 Introduction

Very low-energy radiative capture and weak capture reactions involving few-nucleon systems have considerable astrophysical relevance for the studies of stellar structure evolution and big-bang nucleosynthesis. The radiative capture of neutrons and protons by deuterons, the inverse reactions, and the photodisintegration of ^3H and ^3He , have been investigated experimentally and theoretically over the last decades with some interest. The low-energy behavior of the cross section for the reaction $d(p,\gamma)^3\text{He}$ has important astrophysical implications. This reaction is an essential part of the deuterium burning phase of proto-stellar evolution [1]. It is Step two in the proton-proton chain for burning hydrogen into helium at higher temperatures. Due to the Coulomb barrier of the entrance channel, the cross section drops nearly exponentially with a decrease in the center-of-mass energy, thus becoming increasingly difficult to measure it at the relevant energy at which the reaction takes place in astrophysics. Instead, one was forced to extrapolate high energy cross section data to stellar energies using the astrophysical $S(E)$ factor. The NACRE Collaboration [2] obtained $S(0)$ to be $(0.20 \pm 0.07) \text{ eV}\cdot\text{b}$ and the LUNA Collaboration [3] obtained the cross sections and S -factors for energies below about 20 keV. An analysis of the existing data reported a value of $(0.162 \pm 0.019) \text{ eV}\cdot\text{b}$ for $S(0)$ [4]. Low-energy cross sections, S -factors and thermonuclear reaction rates are also reported and

compared with other measurements and theory [5].

The theoretical description of proton-deuteron radiative capture at low-energies is complicated by the presence of the Coulomb interaction. Only relatively recently has the S -wave capture contribution to the zero-energy S -factor of this reaction been calculated with numerically converged Faddeev wave functions, obtained from the realistic Hamiltonian including the Coulomb interaction. A calculation of the M_1 contribution to $S(0)$ is reported to be $(0.108 \pm 0.004) \text{ eV}\cdot\text{b}$ where the given uncertainty is somewhat subjective [6]. By R -matrix analysis $S(0)$ is found to be $(0.223 \pm 0.010) \text{ eV}\cdot\text{b}$. The R -matrix analysis has the M_1 multipole slightly larger than the $E1$ multipole for E_{cm} less than 10 keV and with $E1$ being dominant for energies above 10 keV. The M_1 contribution to $S(E)$ is nearly flat from zero energy to around 100 keV [7]. In a study of the electromagnetic properties of two- and three-nucleon nuclei, the pair-correlated hyperspherical harmonics method was used with modern two- and three-body interactions and currents to calculate among other things the S -factor for low-energy proton-deuteron radiative capture [8]. The results are in agreement with the LUNA data as well as some older data. The obtained value of $S(0)$ is $0.219 \text{ eV}\cdot\text{b}$.

The nuclear effective field theory (EFT) has been applied to two-, three-, and four-nucleon systems [9–17] in past years. The pionless EFT would be an ideal tool to calculate low-energy cross sections in a model-independent way and to possibly, reduce the theoretical

Received 21 May 2012

1) E-mail: H-Sadeghi@Araku.ac.ir

©2013 Chinese Physical Society and the Institute of High Energy Physics of the Chinese Academy of Sciences and the Institute of Modern Physics of the Chinese Academy of Sciences and IOP Publishing Ltd

errors in a precision calculation. We also suggested a method for the computation of neutron-deuteron radiative capture and triton electromagnetic structure for low-energy with pionless EFT [18–22].

The purpose of the present paper is to study the astrophysical $S(E)$ factor of the $d(p,\gamma)^3\text{He}$ reaction with pionless EFT. At these energies, magnetic transition M_1 gives the dominant contribution. The M_1 amplitude is calculated up to the leading order (LO) with the insertion of a three-body force. The results are in good agreement in comparison with the available experimental data and theoretical calculations at low-energies.

This article is organized as follows. In the next section, a brief description of the relevant Lagrangian and

integral equations are reported. Then the formalism for the total cross section of the proton-deuteron radiative capture and the astrophysical $S(E)$ factor will be presented in section 2. We discuss the theoretical errors, tabulation of the calculated data for $S(0)$ in comparison with the other theoretical approaches and the newly available experimental data in Section 3. Finally, the summary and conclusions follow in Section 4.

2 Brief formalism of Lagrangian and integral equations

We use the three-nucleon Lagrangian [16]

$$\begin{aligned} \mathcal{L} = & N^\dagger \left(iD_0 + \frac{\mathbf{D}^2}{2M_N} \right) N - d^{i\dagger} \left[\sigma_d + \left(iD_0 + \frac{\mathbf{D}^2}{4M_N} \right) \right] d^i - t^{A\dagger} \left[\sigma_t + \left(iD_0 + \frac{\mathbf{D}^2}{4M_N} \right) \right] t^A + y_d [d^{i\dagger} (N^T P(^3S_1) N) + \text{h.c.}] \\ & + y_t [t^{A\dagger} (N^T P(^1S_0) N) + \text{h.c.}] + \mathcal{L}_B + \mathcal{L}_{\text{Three-Body}}, \end{aligned} \quad (1)$$

where M_N , N , d^i and t^A are the nucleon mass, the nucleon field, two dibaryon fields corresponding to the deuteron and the spin-singlet virtual bound state in S -wave nucleon–nucleon scattering, respectively. The projection operators are:

$$P(^3S_1) = \frac{1}{\sqrt{8}} \sigma^2 \sigma^i \tau^2, \quad P(^1S_0) = \frac{1}{\sqrt{8}} \sigma^2 \tau^2 \tau^A, \quad (2)$$

with $\vec{\sigma}$ ($\vec{\tau}$) operating in spin (isospin) space, project out the 3S_1 and 1S_0 NN partial waves, respectively. The $D_\mu = \partial_\mu + ieA_\mu \cdot \hat{Q}$ is covariant derivative, where \hat{Q} is the charge operator. Furthermore, we have the kinetic and gauge fixing terms for the photons,

$$\begin{aligned} \mathcal{L}_B = & \frac{e}{2M_N} N^\dagger (k_0 + k_1 \tau^3) \sigma \cdot B \\ & + e \frac{L_1}{M_N \sqrt{r(^1S_0) r(^3S_1)}} d_t^{j\dagger} d_{s3} B_j + \text{h.c.} \end{aligned} \quad (3)$$

where $k_0 = 1/2(k_p + k_n) = 0.4399$ and $k_1 = 1/2(k_p - k_n) = 2.35294$ are the iso-scalar and iso-vector nucleon magnetic moment in nuclear magnetons, respectively. The unknown coefficient L_1 , will be fixed at its leading non-vanishing order by the thermal cross section [23]. In the doublet-channel of the three-nucleon system, a three-body contact interaction is required for renormalization at leading order [11]. It can be written as

$$\begin{aligned} \mathcal{H}(E; \Lambda) = & \frac{2}{\Lambda^2} \sum_{n=0}^{\infty} \mathcal{H}_{2n}(\Lambda) \left(\frac{ME + \gamma_t^2}{\Lambda^2} \right)^n \\ = & \frac{2\mathcal{H}_0(\Lambda)}{\Lambda^2} + \frac{2\mathcal{H}_2(\Lambda)}{\Lambda^4} (ME + \gamma_t^2) + \dots \end{aligned} \quad (4)$$

where Λ is a momentum cutoff applied in the three-body equations discussed below and $H(\Lambda)$ a known log-

periodic function of the cutoff that depends on a three-body parameter Λ_* . The deuteron wave function renormalization constant is given as the residue at the bound state pole:

$$Z_0^{-1} = i \frac{\partial}{\partial p_0} \frac{1}{i\Delta_d(p)} \Big|_{p_0 = -\frac{\gamma_d^2}{M_N}, \mathbf{p}=0}. \quad (5)$$

The electromagnetic interaction breaks the isospin symmetry that is implicit in the dibaryon propagators from the previous subsection. For the pp-part of the singlet dibaryon we can also have Coulomb photon exchanges inside the nucleon bubble. The result for the leading order propagator is [17]

$$i\Delta_{t,pp}^{\text{AB}}(p) = -\frac{4\pi i}{M_N y_t^2} \frac{\delta^{\text{AB}}}{-1/a_C - 2\kappa H(\kappa/p')}, \quad \kappa = \frac{\alpha M_N}{2}, \quad (6)$$

where $p' = i\sqrt{\mathbf{p}^2/4 - M_N p_0 - i\epsilon}$ and

$$H(\eta) = \psi(i\eta) + \frac{1}{2i\eta} - \log(i\eta), \quad (7)$$

where ψ denotes the logarithmic derivative of the Γ -function. The power counting of pionless effective field theory by definition of the low-energy scale Q of the theory is set by the deuteron binding momentum $\gamma \sim 45$ MeV and including Coulomb photons are introduced in Ref. [16].

For a three-body bound state, we have all the ingredients to discuss the proton-deuteron system in the doublet channel, where the spins of the nucleon and the deuteron couple to a total spin of $1/2$. The spin-singlet dibaryon can now appear in the intermediate state, which leads to two coupled amplitudes that differ in the type of the outgoing dibaryon. In contrast to the quartet channel, the

three nucleon spins no longer need to be aligned in the same direction, which means that a non-derivative three-nucleon interaction is no longer prohibited by the Pauli principle. The diagrams contributing to proton-deuteron radiative capture and scattering that include Coulomb photons are shown in Fig. 1 and Fig. 2. For the low-momentum $p \ll Q$ calculation, diagram (a) simply scales as α/p^2 . The diagram (b) is enhanced relative to (a) by a factor Λ/Q from the nucleon bubble and hence gives the leading order Coulomb contribution. Diagram (a) enters only at the NLO since the dibaryon kinetic energy operators, which generate the direct coupling of the photons to the dibaryons, enter only as effective range corrections. We iterate the diagrams (a) and (b) to all orders and do not include any of the other diagrams shown in Fig. 1.

The claim is that this procedure is adequate for both the quartet-channel and the doublet-channel system. In order to include the Coulomb effects and hence discuss proton-deuteron scattering, we follow [16]. Finally, we have all the ingredients to discuss the proton-deuteron radiative capture. The electromagnetic interaction does not couple to isospin eigenstates, thus we need two different projections for the amplitude \mathcal{T}^b with the outgoing spin-singlet dibaryon [16]:

$$\mathcal{T}_{\text{full}}^{d,b1} = \frac{1}{3}(\sigma^i)_{\alpha'}^{\alpha} (\mathcal{T}_{\text{full}}^{b,iB})_{\alpha'a}^{\beta\beta'} (1 \cdot \delta^{B3})_{b'}^b \Big|_{\substack{a=b=1 \\ \alpha=\beta=1}}, \quad (8)$$

$$\mathcal{T}_{\text{full}}^{d,b2} = \frac{1}{3}(\sigma^i)_{\alpha'}^{\alpha} (\mathcal{T}_{\text{full}}^{b,iB})_{\alpha'a}^{\beta\beta'} (1 \cdot \delta^{B1} + i1 \cdot \delta^{B2})_{b'}^b \Big|_{\substack{a=1, b=2 \\ \alpha=\beta=1}}. \quad (9)$$

$$\begin{aligned} \begin{pmatrix} \mathcal{T}_{\text{full}}^{d,a} \\ \mathcal{T}_{\text{full}}^{d,b1} \\ \mathcal{T}_{\text{full}}^{d,b2} \end{pmatrix} &= \begin{pmatrix} g_{\text{dd}} \left(K_s + \frac{2H(\Lambda)}{\Lambda^2} \right) \\ -g_{\text{dt}} \left(K_s + \frac{2H(\Lambda)}{3\Lambda^2} \right) \\ -g_{\text{dt}} \left(2K_s + \frac{4H(\Lambda)}{3\Lambda^2} \right) \end{pmatrix} + \begin{pmatrix} g_{\text{dd}} K_c^d \\ 0 \\ 0 \end{pmatrix} + \begin{pmatrix} -g_{\text{dd}} D_d \left(K_s + \frac{2H(\Lambda)}{\Lambda^2} \right) & g_{\text{dt}} D_t \left(3K_s + \frac{2H(\Lambda)}{\Lambda^2} \right) & 0 \\ g_{\text{dt}} D_d \left(K_s + \frac{2H(\Lambda)}{3\Lambda^2} \right) & g_{\text{tt}} D_t \left(K_s + \frac{2H(\Lambda)}{\Lambda^2} \right) & 0 \\ g_{\text{dt}} D_d \left(2K_s + \frac{4H(\Lambda)}{3\Lambda^2} \right) & -g_{\text{tt}} D_t \left(2K_s + \frac{4H(\Lambda)}{\Lambda^2} \right) & 0 \end{pmatrix} \otimes \begin{pmatrix} \mathcal{T}_{\text{full}}^{d,a} \\ \mathcal{T}_{\text{full}}^{d,b1} \\ \mathcal{T}_{\text{full}}^{d,b2} \end{pmatrix} \\ &+ \begin{pmatrix} -g_{\text{dd}} D_d K_c^d & 0 & g_{\text{dt}} D_t^{\text{pp}} \left(3K_s + \frac{2H(\Lambda)}{\Lambda^2} \right) \\ 0 & -g_{\text{tt}} D_t K_c^t & -g_{\text{tt}} D_t^{\text{pp}} \left(K_s + \frac{2H(\Lambda)}{\Lambda^2} \right) \\ 0 & 0 & 0 \end{pmatrix} \otimes \begin{pmatrix} \mathcal{T}_{\text{full}}^{d,a} \\ \mathcal{T}_{\text{full}}^{d,b1} \\ \mathcal{T}_{\text{full}}^{d,b2} \end{pmatrix}, \quad (10) \end{aligned}$$

where $D_t^{\text{pp}}(E; q) \equiv \Delta_{t,\text{pp}} \left(E - \frac{q^2}{2M_N}, q \right)$.

The spin structure of the matrix elements of $\text{pd} \rightarrow {}^3\text{He}\gamma$ process is complicated, but in very low-energy for this reaction we can introduce three multiple transitions that can be allowed by p-parity and angular momentum conservation i.e. [18] $J^p = \frac{1}{2}^+ \rightarrow M_1$ and $J^p = \frac{3}{2}^+ \rightarrow M_1, E_2$. The parametrization of the corresponding contribution to the matrix element can be built by the following contributions:

$$\begin{aligned} &i(t^\dagger N)(\vec{D} \cdot [\vec{e}^* \times \vec{k}]), \\ &(t^\dagger \sigma_a N)(\vec{D} \times [\vec{e}^* \times \vec{k}])_a, \\ &t^\dagger (\vec{\sigma} \cdot \vec{e}^* \vec{D} \cdot \vec{k} + \vec{\sigma} \cdot \vec{k} \vec{D} \cdot \vec{e}^*) N, \end{aligned} \quad (11)$$

where N , t , \vec{e} , \vec{D} and \vec{k} are the 2-component spinors of initial nucleon field, the final ${}^3\text{He}$ field, the 3-vector polarization of the produced photon, the 3-vector polarization of deuteron and the unit vector along the 3-momentum of the photons, respectively. The two struc-

tures in Eq. (11) correspond to the M_1 transition. The electric transition E_i^{LSJ} for energies of less than 60 keV dose not contribute to the total cross section. Therefore the $E_2^{0(3/2)(3/2)}$ transition will not be considered in energies relevant to the big-bang nucleosynthesis (BBN) calculation. The M_1 amplitude receives contributions from the magnetic moments of the nucleon and dibaryon operators coupling to the magnetic field, which are described by the lagrange density involving fields Eq. (3). The radiative capture cross section $\text{nd} \rightarrow {}^3\text{He}\gamma$ at very low-energy is given by

$$\sigma = \frac{2}{9} \frac{\alpha}{v_{\text{rel}}} \frac{p^3}{4M_N^2} \sum_{i\text{LSJ}} [|\tilde{\chi}_i^{\text{LSJ}}|^2], \quad (12)$$

where

$$\tilde{\chi}_i^{\text{LSJ}} = \frac{\sqrt{6\pi}}{p\mu_N} \sqrt{4\pi} \chi_i^{\text{LSJ}}, \quad (13)$$

with χ standing for either the electric or magnetic transition and μ_N being in nuclear magneton and p being the momentum of the incident neutron in the center of mass. There is an infinite number of diagrams contributing at

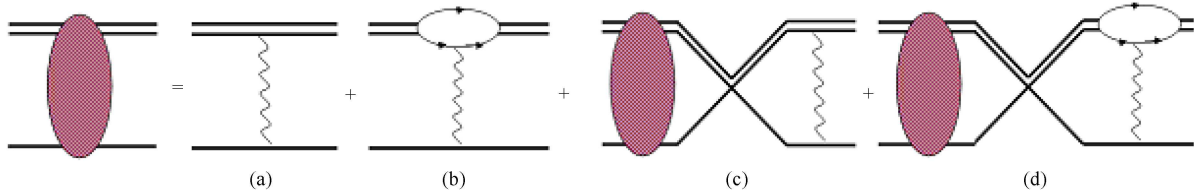


Fig. 1. The Faddeev equation for pd-scattering up to the LO. The thick solid line is the propagator of the two intermediate auxiliary fields D_s and D_t , the propagator of the exchanged nucleon and the wavy lines denote the virtual photons.

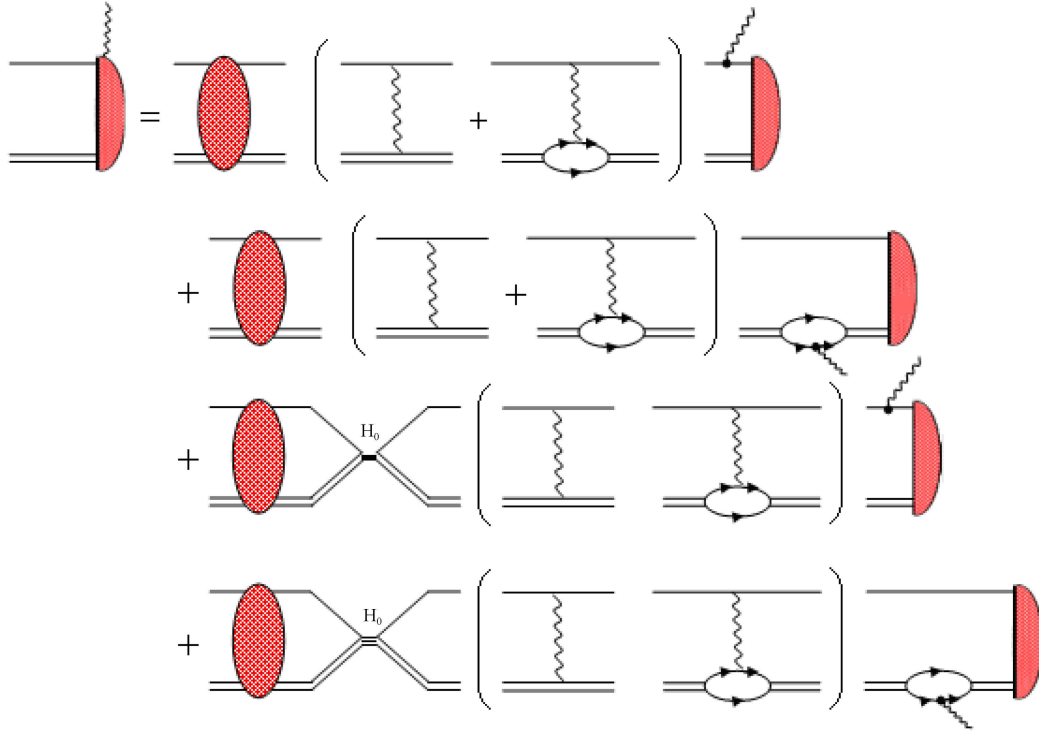


Fig. 2. The Faddeev equation for pd-radiative capture up to the LO. The circles indicate the insertion of pd-scattering amplitude up to the LO from Fig. 1 (only up to the first line of perturbative expansion of the Faddeev equation). The three-body interactions are shown with strength $H_0(\Lambda)$. The wavy line shows photon and small circles show the magnetic photon interaction. The photon is minimally coupled. The semi-circles show the final triton bound state. The remaining notation is shown as in Fig. 1.

Table 1. Results for the cutoff variation of the cross section up to the LO are shown between $\Lambda=150$ MeV and $\Lambda=500$ MeV.

$E/(10^{-8}$ MeV)	LO
1	0.0008
2	0.0011
2.65	0.0014
3	0.0017
10	0.0026

the leading order for M_1 amplitude of the radiative capture cross section $pd \rightarrow {}^3\text{H}\gamma$, as shown in Fig. 2. We follow the same procedure as [18].

As we are interested only in the ultra-violet (UV)

behavior, i.e. in the asymptote, and no infra-red (IR) divergences occur, we can safely neglect the IR limit of the integral. All calculations were performed with the cutoff at 400 MeV. The results are shown in Table 1. For the energy range of our calculation, below the break-up reaction, we show cutoff variation of the cross section between $\Lambda=150$ MeV and $\Lambda=500$ MeV as a function of the center-of-mass energy. We confirm that in our calculation also in a very low-energy range, the cutoff variation has a very smooth slope.

3 Results and discussion

We numerically solved the Faddeev integral equation

up to the LO. We used $\hbar c = 197.327$ MeVfm, a nucleon mass of $M_N = 938.918$ MeV, for the NN triplet channel a deuteron binding energy (momentum) of $B = 2.225$ MeV ($\gamma_d = 45.7066$ MeV). The proton-proton Coulomb scattering length $a_C = -7.8063 \pm 0.0026$ fm [24]. The remaining parameters can be found in Ref. [18].

The astrophysical S factor of the ${}^2\text{H}(p, \gamma){}^3\text{He}$ radiative capture reaction at thermal energy is given by:

$$S(E) = E\sigma_t(E)e^{2\pi\alpha/v}, \quad (14)$$

where E is the pd center of mass kinetic energy, $\sigma_t(E)$ is the total cross section, α is the fine structure constant, and v is the pd relative velocity.

The results for $S(0)$ are summarized in Table 2. The experimental data are from Refs. [1, 25–27].

Table 2. Comparison between different results for the astrophysical $S(0)$ factor of the reaction proton-deuteron radiative capture at zero energy. The last line shows our result using EFT at LO order.

research group	$S(0)/(\text{eV}\cdot\text{b})$
Schiavilla et al. [27]	0.185 ± 0.005
Griffiths et al. [25]	0.25 ± 0.04
Schimd et al. [26]	0.166 ± 0.014
LUNA Collaboration [3]	0.216 ± 0.010
EFT(LO)	0.243

Here, no significant difference has been seen between the results obtained with the present model based on pionless EFT, the nuclear current operator, the modern nucleon-nucleon potential model and experimental results. The agreement between the theoretical predictions and the experimental data, especially the very recent LUNA data [1], is good. In particular, the calculated S -factor at zero energy is 0.243, which is in agreement with the LUNA and Griffiths results. The most complete comparison between EFT and the AV18/UIX interaction [27], with a nuclear electromagnetic current operator that includes both one- and two-body contributions, for the astrophysical S -factor at zero energy was also performed. The EFT result is closest to the experimental result.

We also compare the predictions obtained with pionless EFT with other available experimental results. The calculated S -factor in the energy range 0–1 MeV is compared with the experimental data of Refs. [25, 26, 28] in Fig. 3. For very low-energies, the results are in good agreement with the Huang, LUNA and Griffiths results [25, 26, 28].

The results for $S(0)$ show that the P -wave capture channels are very important at higher energies. The energy dependence of the astrophysical $S(E)$ suggests higher partial waves and higher order calculations at higher energies. It should be noted that the E_1 opera-

tor makes a small contribution to the total cross section above 1 MeV in comparison with M_1 .

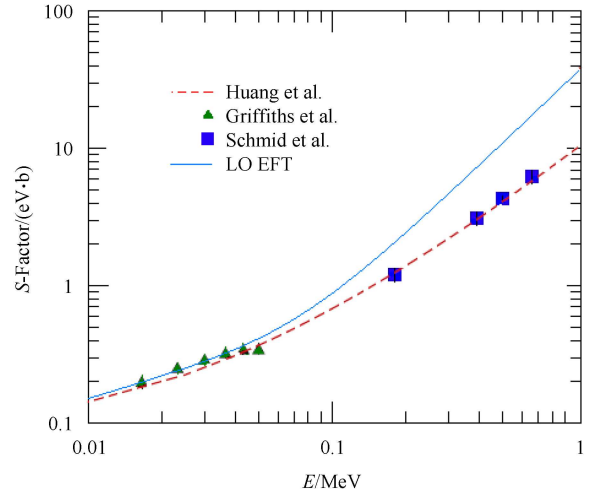


Fig. 3. The calculated S -factor for $d(p, \gamma){}^3\text{He}$ obtained using EFT up to LO is compared with the available experimental data. Experimental data are taken from Refs. [25, 26, 28].

The strength of the EFT calculation is that it allows for the estimation of the theoretical uncertainties of a calculation because contributions to the scattering amplitudes are ordered by a small expansion parameter Q . $N^n\text{LO}$ corrections to $k\cot\delta$ should typically be of the order $\Delta(k\cot\delta) \sim Q^n = \left(\frac{p}{\Lambda}\right)^n$ compared with the LO result. A typical low-momentum scale p in the three-body system is the binding momenta of the two-nucleon bound state, $\gamma \approx 45$ MeV. The breakdown scale $\Lambda \approx m_\pi$ of the theory is the scale at which higher-order corrections become comparable in size. Like the actual size of the expansion parameter Q , its value must be verified in actual calculations. By considering $Q \approx \frac{1}{3}$ in pionless EFT of nuclear physics, the theoretical accuracy by neglecting higher-order terms is here estimated conservatively by $Q \approx \frac{1}{3}$ of the difference between the NLO- and N2LO-result [29].

4 Summery and conclusion

Understanding the nature of ${}^3\text{He}$, the only stable 3-body nucleus, constitutes a major advance toward the solution to the general problem of nuclear forces. In particular, it involves the influence of the third nucleon on the interaction between the other two. We have investigated the approach for constructing electromagnetic currents by using minimal substitution in the two- and three-nucleon interactions.

The zero energy astrophysical $S(0)$ factor for the thermal proton radiative capture by deuteron is calculated with pionless EFT. The astrophysical $S(0)$ factor is accurately determined to be $S(0)=0.243$ eV·b up to the leading order (LO). At zero energies, the magnetic transition M_1 gives the dominant contribution. The M_1 amplitude is calculated up to the LO. A good quantitative

agreement between the theoretical and experimental results is found for all observables. The demonstrations of the cutoff independent calculation have also been presented. For the ^3He nuclear systems, the cross sections as well as the astrophysical S -factor have been calculated and compared with the corresponding experimental results in the energy range 0–1 MeV.

References

- 1 Descouvemont P et al. Nucl. Phys. A, 2005, **758**: 783c
- 2 Angulo C et al. Nucl. Phys. A, 1999, **656**: 3
- 3 Casella C et al. Nucl. Phys. A, 2002, **706**: 203
- 4 Artemov S V et al. Izv. Ross. Akad. Nauk. Ser. Fiz., 2009, **73**: 176; Bull. Russ. Acad. Sci. Phys., 2009, **73**: 165
- 5 MA L et al. Phys. Rev. C, 1997, **55**: 588
- 6 Friar J L et al. Phys. Rev. Lett., 1991, **66**: 1827
- 7 Descouvemont P et al. Data Nucl. Data Tables, 2004, **88**: 203
- 8 Marcucci L E et al. Phys. Rev. C, 2005, **72**: 014001
- 9 Kaplan D B, Savage M J, Wise M B. Nucl. Phys. B, 1998, **534**: 329
- 10 Beane S R, Savage M J. Nucl. Phys. A, 2001, **694**: 511
- 11 Bedaque P F, Hammer H W, van Kolck U. Phys. Rev. Lett., 1999, **82**: 463; Nucl. Phys. A, 1999, **646**: 444
- 12 Bedaque P F, Hammer H W, van Kolck U. Nucl. Phys. A, 2000, **676**: 357
- 13 Hammer H W, Mehen T. Phys. Lett. B, 2001, **516**: 353
- 14 Bedaque P F, Griebhammer H W. Nucl. Phys. A, 2000, **671**: 357
- 15 Gabbiani F, Bedaque P F, Griebhammer H W. Nucl. Phys. A, 2000, **675**: 601
- 16 Konig S, Hammer H W. Phys. Rev. C, 2011, **83**: 064001
- 17 Ando S, Birse M C J. Phys. G: Nucl. Part. Phys., 2010, **37**: 105108
- 18 Sadeghi H, Bayegan S. Nucl. Phys. A, 2005, **753**: 291
- 19 Sadeghi H, Bayegan S, Griebhammer H W. Phys. Lett. B, 2006, **643**: 263
- 20 Sadeghi H. Phys. Rev. C, 2007, **75**: 044002
- 21 Sadeghi H, Bayegan S. Few-Body Systems, 2010, **47**: 167
- 22 Sadeghi H, Nezamdost J. Prog. Theor. Phys., 2010, **124**: 1037
- 23 CHEN J W, Rupak G, Savage M J. Phys. Lett. B, 1999, **464**: 1
- 24 Bergervoet J R et al. Phys. Rev. C, 1988, **38**: 770
- 25 Griffiths G M, Larson E A, Robertson L P. Can. J. Phys., 1962, **40**: 402
- 26 Schmid G J et al. Phys. Rev. C, 1995, **52**: R1732
- 27 Schiavilla R, Viviani M, Kievsky A. Phys. Rev. C, 1996, **54**: 553
- 28 HUANG J T, Bertulani C A, Guimaraes. Atomic Data and Nucl. Data Tables, 2010, **96**: 824847
- 29 Griebhammer H W. Nucl. Phys. A, 2004, **744**: 192